Nanocrystalline Metal Oxides as Destructive Adsorbents for Organophosphorus Compounds at Ambient Temperatures

Shyamala Rajagopalan,[a] Olga Koper,[a] Shawn Decker,[a] and Kenneth J. Klabunde*[a, b]

Abstract: Nanocrystals of magnesium oxide react with organophosphorus compounds at room temperature by dissociative chemisorption, which we term "destructive adsorption". This process involves cleavage of P–O and P–F bonds (but not P–C bonds) and immobilization of the resultant molecular fragments. These ultrafine powders have unusual crystalline shapes and possess high surface concentrations of reactive edge/corner and defect sites, and thereby display higher surface reactivity, normalized for surface area, than typical polycrystalline material. This high surface reactivity coupled with high surface area allows their use for effective decontamination of chemical warfare agents and related toxic substances. Herein data is presented for paraoxon, diisopropylfluorophosphate (DFP), and $(CH_3CH_2O)_2P(O)CH_2SC_6H_5$ (DEPTMP). Solid-state NMR and IR spectroscopy indicate that all OR and F groups dissociate; this leaves bound $-PO_4$, $-F$, and $-OR$ groups for paraoxon, DFP, and DEPTMP, respectively. For paraoxon, it was shown that one monolayer reacts. For DEPTMP, the OR groups dissociate, but not the $P-CH_2SC_6H_5$ group. The nanocrystalline MgO reacts much faster and in higher capacity than typical activated carbon samples, which physisorb but do not destructively adsorb these phosphorous compounds.

Keywords: adsorption · decontamination · MgO · organophosphorus compounds · solid-state reactions

Introduction

Nanocrystalline materials exhibit a wide array of unusual properties, and can be considered as new materials that bridge molecular and condensed matter.[1] One of the unusual features is enhanced surface chemical reactivity (normalized for surface area) toward incoming adsorbates.[2] For example, 4 nm MgO crystals adsorb more than three times as much SO_2 or CO_2 per nm^2 than more conventional material, and many times more than commercially available common MgO.[3] Similarly, nano-MgO, CaO, and Al_2O_3 adsorb polar organics such as aldehydes, alcohols, ketones, and other polar organics in very high capacities, and substantially outperform the activated carbon samples that are normally employed for such purposes.[4] Indeed, nanocrystalline oxides in powder or porous pellet forms make up a family of very powerful adsorbents.[5]

Herein we report studies aimed at determining if these ionic, nontoxic materials would be capable of destructive adsorption of organophosphorus reagents at room temperature or below.[6–9] Previous work at *elevated* temperature ($>300\,^{\circ}C$) has shown that organophosphorous compounds are effectively mineralized by these nanomaterials;[6] while NMR studies of nanocrystalline MgO, CaO, and Al_2O_3 interacting at room temperature with VX, HD, and GD (chemical warfare agents) have been promising and indicate that the products are nontoxic.[7]

[a] Prof. K. J. Klabunde, Chief Tech. Officer Dr. S. Rajagopalan, Dr. O. Koper, Dr. S. Decker
Nanoscale Materials, Inc., 1500 Hayes Drive
Manhattan, KS 66502 (USA)
E-mail: kenjk@ksu.edu

[b] Prof. K. J. Klabunde
Department of Chemistry, Kansas State University
Manhattan, KS 66506 (USA)
Fax: (+1) 913-532-6666

Experimental Section

Commercial oxides were purchased from Fisher Scientific or Aldrich. Conventionally prepared (CP) oxides such as CP-MgO were prepared as previously described, as were aerogel oxides such as AP-MgO (nanocrystalline materials).[8] These preparation methods involved a final heat treatment under vacuum at $500\,^{\circ}C$. The oxides were stored under nitrogen, but can be handled in air during experimental manipulations. Paraoxon and DFP were purchased from Aldrich, and DEPTMP was purchased from Lancaster; all three were used as received. Activated carbon samples were purchased from Aldrich.

Samples for FTIR analysis were prepared by grinding a sample of the vacuum-dried solid (1 to 3 mg) with anhydrous KBr (100 mg). Pellets were made with a standard pellet press. IR spectra of neat liquids were obtained by spreading a thin film of the liquid between a pair of salt plates. ^{31}P NMR spectra were obtained by using a Tecmag 270 MHz spectrometer equipped with a Doty Scientific 7 mm high-speed CP-MAS probe, and by using direct excitation and high power proton decoupling.[10] The observation frequency for ^{31}P was 109.55 MHz. Samples were packed in a sapphire rotor with kel-F end caps and typically spun at 4700 Hz. Chemical shifts were referenced to external 85 % H_3PO_4 ($\delta = 0$ ppm). ^{13}C MAS NMR spectra were obtained

  0947-6539/02/0811-2602 $ 20.00+.50/0 *Chem. Eur. J.* **2002**, *8*, No. 11

on a Chemagnetics CMX-300 model 300 MHz spectrometer with an observation frequency of 75 MHz. Samples were spun at 8000 Hz. Chemical shifts were referenced to external TMS ($\delta = 0$ ppm)

Room-temperature destructive adsorption of paraoxon [$(CH_3CH_2O)_2P(O)OC_6H_4NO_2$] and DEPTMP [$(CH_3CH_2O)_2P(O)CH_2SC_6H_5$]: Adsorbents examined in this study included aerogel-prepared magnesium oxide (AP-MgO), conventionally prepared magnesium oxide (CP-MgO), commercially available magnesium oxide (CM-MgO), activated carbons from norite (AC-NO), Darco (AC-DA), coconut shell (AC-CO), and Ambersorb(R)572 (AM).

Adsorbent (100 or 200 mg) was placed in a 250 mL round-bottom flask equipped with a magnetic stirrer, and pentane (100 or 200 mL) was added. The solution was purged with nitrogen to remove any oxygen, and then the organophosphorus compound (4.5 or 9 μL) was added and its disappearance was monitored by UV/Vis spectroscopy (about 5×10^{-7} M detection limit). The data were taken after 2, 5, 10, 15, and 20 minutes, then every 20 minutes up to 2 h. After overnight reaction, the solid was separated, vacuum dried, and studied by transmission IR and NMR spectroscopy.

In some cases the spent oxides and activated carbon were extracted with toluene, CH_2Cl_2, or CH_3OH. For example, an excess of toluene was added and the samples were sonicated for 20 minutes to ensure proper extraction. After that time, the GC-MS spectra of the extracts were taken on a Hewlett–Packard GC-MS. In the case of AP-MgO, no paraoxon or other organic residue was extracted, whereas in the activated carbon cases, paraoxon was obtained in significant amounts.

Room temperature destructive adsorption of DFP, [$(Me_2CHO)_2P(O)F$]: Adsorbents examined in this study included AP-MgO, CP-MgO, and CM-MgO. The adsorbents were evacuated at room temperature for ≈15–30 min (≈10^{-4} Torr) prior to adsorption. In a typical experiment, the adsorbent (100 mg) was weighed into a vapor-phase IR cell that could be connected to a vacuum line. After this treatment, a background spectrum was recorded. Subsequently, DFP was introduced (9 μL, ≈5 wt %) into the sample cell and the IR spectrum of the vapor phase was recorded after 1 h. In order to assess the structure of the adsorbed species, reaction with DFP was carried out as described below, and the DFP adsorbed on the solid was isolated and analyzed.

In a representative experiment, a 250 mL single necked flask with a serum cap, a stir bar, and a magnetic stirrer was charged with dry pentane (200 mL). The solid adsorbent (200 mg) and DFP (9 μL, ≈5 wt %) were added sequentially to the flask. After an hour at room temperature the stirring was stopped, the solvent was decanted, and the solid was dried overnight under vacuum, and analyzed by IR and solid state NMR.

Results

Paraoxon: An array of samples was studied for their ability to destructively adsorb paraoxon. The best adsorbent was nanocrystalline magnesium oxide. The results are given in Figure 1, which shows the disappearance of paraoxon upon exposure to various MgO samples including AP-MgO nanocrystals, CP-MgO microcrystals, and polycrystalline CM-MgO with pentane as the solvent medium.

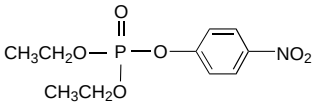

Paraoxon

The AP-MgO nanoparticles outperform all other magnesia samples tested. The paraoxon was *completely adsorbed on the AP-MgO* sample before the first reading could be measured at 2 minutes after exposure. This behavior has been repeated in many test trials and is due to the material's reactive nature and very high surface area of 400–600 $m^2 g^{-1}$; for the studies reported herein, a sample of 400 $m^2 g^{-1}$ was used. The conventionally prepared MgO samples (150 $m^2 g^{-1}$) also adsorbed paraoxon relatively efficiently, while commercially available MgO samples (30 $m^2 g^{-1}$) were not at all effective. In addition, noncoated and coated nanoscale oxides and hydroxides of calcium (aerogel and conventionally prepared), aluminum, and zinc oxide were used. The results were also very promising, although none was as effective as AP-MgO (results not shown). It was also noted that when AP-MgO samples were directly compared with each other, higher surface area samples performed better, as would be expected.

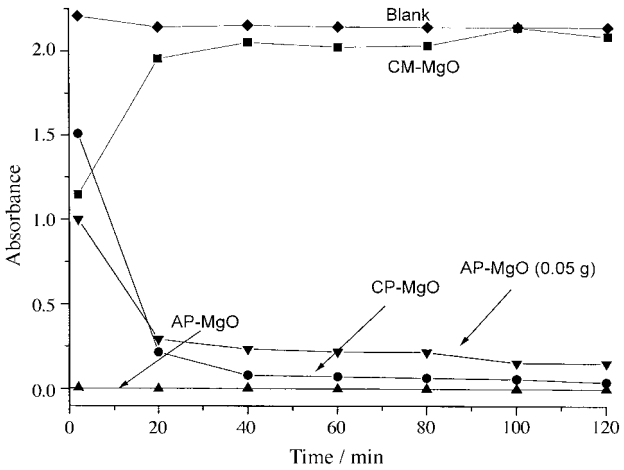

Figure 1. Adsorption of paraoxon (4.5 μL) on magnesium oxide (0.1 g) dispersed in pentane, monitored by UV/Vis spectroscopy (267 nm band). AP samples are nanocrystalline (surface area 400 $m^2 g^{-1}$, crystallite size = 4 nm); CP sample (150 $m^2 g^{-1}$, 8 nm); CM sample (30 $m^2 g^{-1}$, >20 nm).

While evidence of actual destruction of the mimic compound was observed for many of these reactive adsorbents, we were able to confirm that destructive adsorption does *not* take place with activated carbon, a well-known highly adsorbent material. Activated carbon adsorbs paraoxon; but, in contrast to AP-MgO, it could be removed by toluene extraction. An unexpected outcome of the research was that activated carbon actually has a lower adsorption capacity than the AP-MgO material on an equivalent gram basis. When 100 mg of each adsorbent was used, only 4.5 μL of paraoxon was completely adsorbed on the activated carbon surface whereas the AP-MgO adsorbed/destroyed 15 μL of paraoxon. The comparison between activated carbon and AP-MgO is illustrated in Figure 2. In Figure 3a is shown the ^{31}P MAS NMR spectrum of the AP-MgO/paraoxon solid. Five peaks with the center peak at $\delta = 0.85$ ppm are observed. The outer peaks are due to spinning side bonds.

FTIR studies of the solid AP-MgO/paraoxon sample were carried out, and peak assignments were made based on literature.[9] After the adsorption on AP-MgO, a band for OH groups appeared in the IR spectrum; this is probably due in part to adventitious water adsorption during IR sample preparation and handling (KBr pellets were used, as described in the Experimental Section). However, ethoxide dissociation could also have formed some surface −OH and

  0947-6539/02/0811-2603 $ 20.00+.50/0

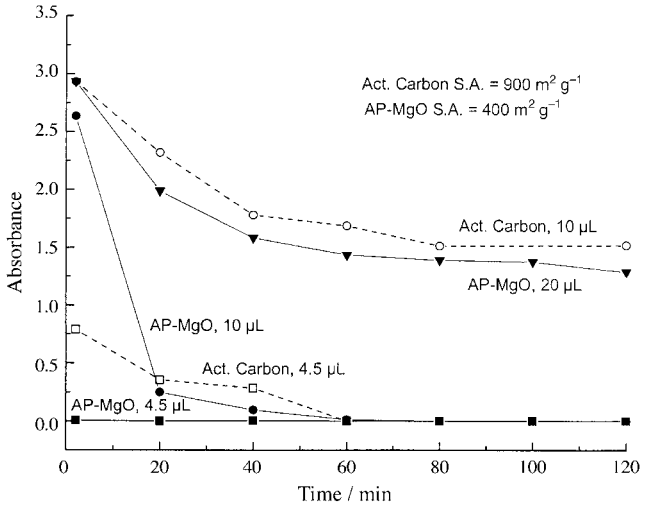

Figure 2. Adsorption of paraoxon on AP-MgO (0.1 g) compared with activated carbon (0.1 g) dispersed in pentane, monitored by UV/Vis spectroscopy (267 nm band).

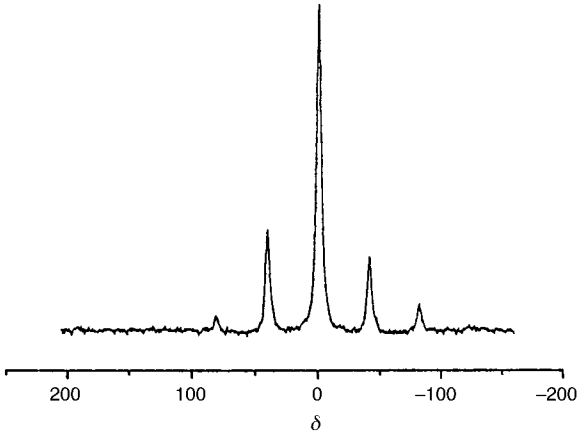

Figure 3. ^{31}P MAS NMR spectra of solid AP-MgO with adsorbed paraoxon.

C_2H_4. The bands due to ring stretching (1594 cm^{-1}, 1494 cm^{-1}) as well as N–O asymmetric stretching at 1525 cm^{-1} broadened and shifted toward lower wavenumbers. A new broad band at 1307 cm^{-1} might be attributed to a symmetric stretch of N–O in $ArNO_2$. The P=O stretching at 1283 cm^{-1} in the neat paraoxon spectrum appears to be almost completely gone, giving way to a very small feature at 1216 cm^{-1}. A very strong band at 1032 cm^{-1} assigned to C-O-(P) stretching in P-O-Et almost completely disappeared; this indicates the dissociation of the ethoxy group from the paraoxon. The interpretation of the spectrum of paraoxon after adsorption on activated carbon is much more difficult, since the spectral features are very broad.

DEPTMP: The UV spectrum of DEPTMP in pentane contains two absorption bands centered around 209 and 256 nm. A series of concentrations allowed construction of a calibration curve, and by using a one-hour exposure time (time elapsed after MgO nanoparticle powder addition) it was determined that AP-MgO, was clearly superior to CP-MgO, CM-MgO, and a series of activated carbon samples and Ambersorb (Table 1).

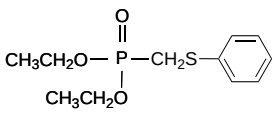

DEPTMP

Table 1. Percentage of DEPTMP adsorbed in one hour for a series of adsorbents.

Adsorbent	Adsorbed[a] [%]
AP-MgO	96
CP-MgO	74
CM-MgO	17
AC-DA[b]	24
AC-NO	35
AC-CO	28
AM	59

[a] Average of 3 or 4 determinations. [b] Use of crushed AC-DA resulted in 47 % adsorbed.

For IR studies, AP-MgO was treated with excess DEPTMP in pentane. After one hour the solid was collected and washed repeatedly with pentane until UV spectra indicated that no more DEPTMP was being removed. The solid was analyzed by FTIR. Although the peaks were broad, alkyl and aryl C–H bands (3100 – 2800 cm^{-1}) did not change much upon adsorption. The $\tilde{\nu}_{P=O}$ band shifted from 1250 cm^{-1} to 1206 cm^{-1}, while a band remaining at 1048 cm^{-1} could be due to $\upsilon_{C\text{-}O\text{-}P}$ or $\upsilon_{C\text{-}O\text{-}Mg}$. Although this band did not shift, there is evidence in the literature that the C–O stretch of some phosphonates does not change much upon adsorption and hydrolysis by inorganic oxides.[6, 11a, 12–14]

Figure 4 shows the ^{31}P MAS NMR spectrum of AP-MgO-adsorbed DEPTMP (5 wt %). It displays two major peaks centered around $\delta = 24.2$ and 15.7 ppm and a set of two smaller peaks, which are attributed to spinning side bands (the ^{31}P NMR shift for neat DEPTMP in $CDCl_3$ is $\delta = 23.4$ ppm). From a literature survey[10] we found that for derivatives of the type $(EtO)_2PO(R)$, where $R = CH_3$, Et, or Bu, ^{31}P NMR delta values ranged from $\delta = 29.6$ to 32.6 ppm. Thus, it appears that the signals observed in the DEPTMP/AP-MgO sample are probably due to an adsorbed species that contains a more

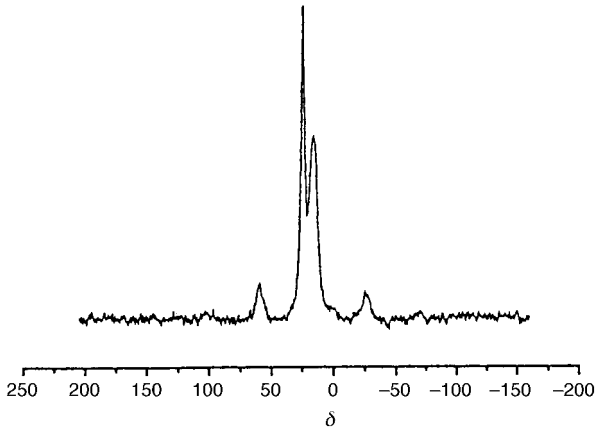

Figure 4. ^{31}P MAS NMR spectra of solid AP-MgO with adsorbed DEPTMP.

0947-6539/02/0811-2604 $ 20.00+.50/0 *Chem. Eur. J.* **2002**, *8*, No. 11

shielded phosphorus nucleus. We assign these two peaks to the mono- and dihydrolyzed species (cleavage of P–OEt bonds, but not cleavage of the P–CH_2 bonds). This assignment is based on the fact that alkoxy groups in paraoxon, DFP, and GD[7a] are readily hydrolyzed. Furthermore, in the work by Wagner et al.[7a] the mono- and dihydrolyzed species are at $\delta = 18.5$ and 25.7 ppm, respectively, which are close to the peaks we observed for the hydrolyzed DEPTMP. Also, upon aging the AP-MgO/DEPTMP sample the peaks at $\delta = 24.2$ (major) and 15.7 (minor) changed slightly to $\delta = 25.0$ and 17.9, respectively. The minor peak also grew; this suggests that it represents the dihydrolyzed species.

DFP: Experiments with DFP were carried out by exposing the reagents to MgO samples under vacuum and analyzing the vapor above the solid by IR spectroscopy. These studies showed that all of the DFP sample was adsorbed from the vapor phase by AP-MgO, whereas CP-MgO and CM-MgO did not completely adsorb the sample. Thus, qualitatively, AP-MgO was a superior adsorbent.

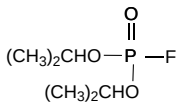

DFP

FTIR spectra of the solid after treatment with DFP showed the appearance of $\tilde{\nu}_{O\text{-}H}$ (3700 – 3000 cm^{-1}). The alkyl C–H stretching region (3100 – 2800 cm^{-1}) did not change much upon adsorption. However, the $\tilde{\nu}_{P=O}$ band shifted from 1298 to 1260 cm^{-1} and was rather weak. The $\tilde{\nu}_{C\text{-}O(P)}$ band did not shift much (1016 cm^{-1}), and characteristic absorptions (1177, 1141, 1110 cm^{-1}) due to "rocking vibrations" of the methyl groups of the isopropyl units were still observed without appreciable shift compared with neat DFP. New prominent bands appeared in the 1100 – 990 cm^{-1} region: an intense peak at 1079 cm^{-1} and a broad absorption at 992 cm^{-1}. We assigned these new bands to a bridged "POO" species. The existence of such structures has been proposed before for other adsorbed organophosphorus agents, such as DMMP/AP-MgO, Sarin/Al_2O_3, Sarin/MgO and DMMP/Al_2O_3 (DMMP = dimethoxymethyl phosphate).[11–14]

The ^{31}P NMR spectrum (Figure 5) showed one set of peaks (with spinning side bands) centered at $\delta = -0.76$ ppm, shifted from $\delta = 11.2$ ppm for neat DFP.[15] This large upfield shift and its symmetrical nature indicate a highly shielded phosphorus nucleus, such as PO_4^{3-}. Indeed, phosphoric acid yields a similar spectrum, and so it appears that DFP was completely hydrolyzed (destructively adsorbed) by AP-MgO. Furthermore, the spectrum is essentially identical, but for a small shift, to that observed for paraoxon ($\delta = 0.85$ ppm) described earlier. *Thus, phosphoric acid, DFP, and paraoxon yield identical NMR peaks except for very small ppm shifts.*

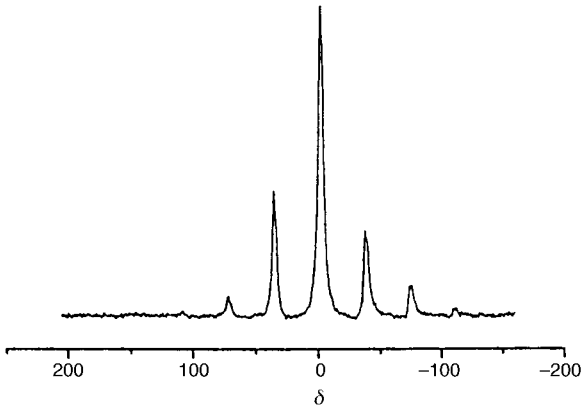

Figure 5. ^{31}P MAS NMR spectra of solid AP-MgO with adsorbed DFP.

We interpret these IR and NMR results as indicating that DFP rapidly adsorbs on the AP-MgO through a bridge "POO" structure with loss of the P–F bond, followed by slower destructive adsorption of the P-O-C bonds.

Discussion

The adsorption ability of nanocrystalline ionic metal oxides, in particular MgO, can be attributed to morphological features—a high proportion of edge/corner sites are available due to their polyhedral shapes. Both Lewis base and Lewis acid sites at edges/corners would be stronger due to coordinative unsaturation. Indeed, models suggest that at least 20% of surface ions are positioned on edge/corners.[1, 2] Furthermore, according to magnetic susceptibility studies, other types of surface defects such as ion vacancies and electron-deficient and electron-rich sites exist.[16]

However, while the residual surface OH groups are certainly relevant,[7, 11] their importance cannot be determined from the data presented here. Further work is planned with the goal of elucidating the importance of certain types of surface OH groups (isolated vs. hydrogen bonded).

Amount and rate of adsorption: It is of interest to determine if AP-MgO has a high capacity for adsorption corrected for surface area, and estimate rate enhancements more quantitatively, compared with more normal forms of MgO and with activated carbon samples.

By using data from Figures 1 and 2, Table 2 was generated. It gives estimates of the rate of paraoxon adsorption in moles

Table 2. Initial rates (first 20 minutes) of paraoxon adsorption from pentane by various adsorbents.

Sample	Surface Area [$m^2 g^{-1}$]	Paraoxon [mol]	Adsorbent [mol]	Adsorbed [%]	Rate [mol per mol adsorbent $min^{-1} m^{-2}$][b]
AP-MgO	400	3.6×10^{-5}	2.5×10^{-3}	92	1.7×10^{-5} (7.5×10^{-2} M $^{-1}$ s^{-1})
CP-MgO	150	1.6×10^{-5}	2.5×10^{-3}	92	1.9×10^{-5}
CM-MgO	30	1.6×10^{-5}	2.5×10^{-3}	0	≈ 0
act. carbon	900	3.6×10^{-5}	8.3×10^{-3}	23	0.05×10^{-5}

[a] At $t = 0$, absorbance taken as 3.0 from Figure 2 and 2.5 from Figure 1. [b] The number in parentheses is a value for homogeneous base hydrolysis of paraoxon.[18, 19]

  0947-6539/02/0811-2605 $ 20.00+.50/0

of paraoxon per minute per mole of adsorbent per m^2, so these values are corrected for surface area. The results indicate that AP-MgO and CP-MgO are comparable in initial rate of adsorption and that both have a much higher rate than activated carbon. This is an interesting finding since it is known that the surface morphologies of AP-MgO (polyhedral, large surface concentration of edges/corners, defects) and CP-MgO (hexagonal platelets) are quite different and sometimes exhibit intrinsically different chemistry.[17]

Figures 1 and 2 are also useful regarding capacity of adsorption. For AP-MgO (100 mg) we note that about 15 μL of paraoxon saturate the surface. This is equivalent to about 0.015 g, 5.5×10^{-5} moles, or 33×10^{18} molecules, which are adsorbed onto 40 m^2 (40×10^{18} nm^2)/0.1 g of MgO, or 0.85 molecules per nm^2. The area taken up by a paraoxon molecule that has dissociated into phenoxide and bridging phosphate moiety can be calculated. It can be estimated that a phenolic ion is about 7.4 Å in length and occupies an area of $0.74 \times 0.74 = 0.55$ nm^2. Similarly, a bridging $[(EtO)_2PO]_{ads}$ fragment (which probably exists as surface-bound PO_4 and OEt groups) would be 6.7 Å in length, that is, $0.67 \times 0.67 = 0.45$ nm^2. Thus, these adsorbed fragments would occupy approximately 1.0 nm^2. So the experimentally adsorbed amount of 0.85 molecules per nm^2 is very close to a monolayer. These calculations translate into moles of AP-MgO to moles of paraoxon = 45:1, and mass of MgO to mass of paraoxon = 6.5:1. Structure **1** shown in Figure 6 is a likely formulation of the surface-bound structures. (It is likely that some of the bound −OEt dissociated to −OH plus C_2H_4, a rather facile process on basic surfaces). The existence of a *p*-nitrophenoxide anion is assumed since, upon adsorption, the solid turns from white to bright yellow, the color of that anion in solution.

In comparison, with activated carbon a similar calculation indicates that at most 7 μL of paraoxon is taken up on 90 $m^2 g^{-1}$, or 15×10^{18} molecules per 90×10^{18} nm^2; this equals 0.17 molecules per nm^2—well below a monolayer.

Another difference between the high surface area MgO sample and carbon samples is that the paraoxon is dissociatively chemisorbed onto MgO whereas, on carbon, physisorption takes place. This idea is supported by the NMR and IR data, and the fact that exhaustive extraction of the spent adsorbent with toluene, CH_2Cl_2, and CH_3OH did not yield an extractable material in the case of AP-MgO, but with activated carbon intact paraoxon was recovered. Furthermore, similar results were obtained when these absorbents were treated with paraoxon in the dry state (no pentane solvent), followed by extraction. So paraoxon and DFP appear to be completely dissociatively chemisorbed (all OR or F groups removed). However, in the case of DEPTMP, the $CH_2SC_6H_5$ group apparently does not dissociate from the phosphorus group. It appears from the ^{31}P MAS NMR that two structures are likely that represent an initial dissociation of one OR group, and then slowly the other OR group (Figure 6, structures **3a** and **b**). Indeed, as described in the Results section, the spectra changed over time, and the peak in the $\delta = 17.9$ ppm region grew; this is the most shielded and probably represents the dihydrolyzed species (structure **3b**).

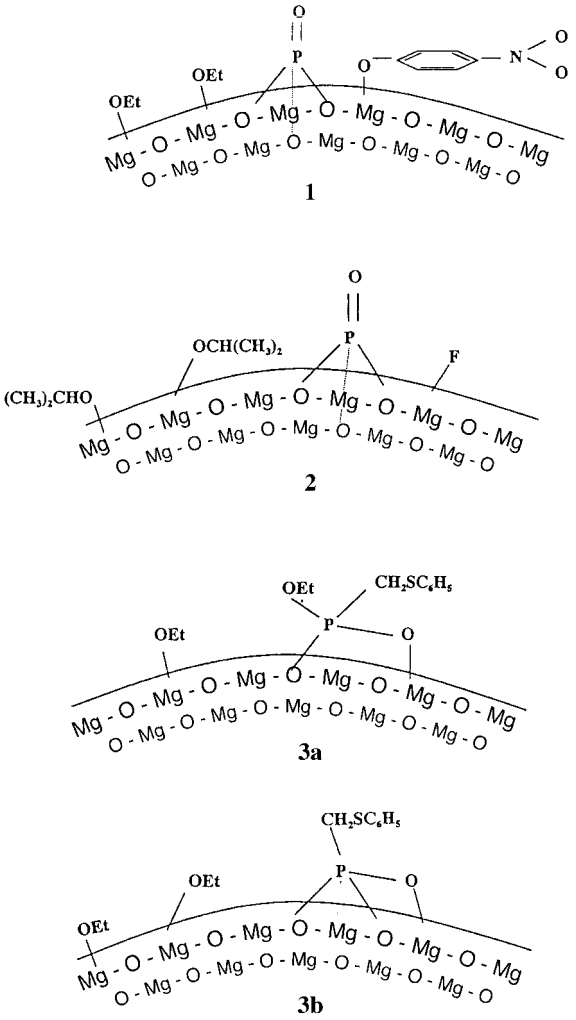

Figure 6. Proposed surface structures for the adsorbed species on AP-MgO; **1** paraoxon, **2** DFP, **3a** and **b** DEPTMP.

Proposed surface structures: The NMR, IR, and solvent extraction data strongly suggest that destructive adsorption takes place. In the case of paraoxon and DFP, the ^{31}P MAS NMR spectra were almost identical and at a shift position nearly the same as for the standard H_3PO_4. These spectra have a single sharp resonance with spinning side bands. This suggests that a PO_4 species is involved, which in turn suggests that all the bound OR groups were dissociated. In Figure 6 we have given general schemes for what the surface species may be.

For the AP-MgO/paraoxon adduct, ^{13}C CP-MAS spectra were also obtained. This sample exhibited two major sets of peaks centered at $\delta = 13.6$ and 60.5 ppm, and these can be assigned to the CH_3 and CH_2 groups of adsorbed OEt. In addition, a set of four peaks in the region of $\delta = 119 - 180$ ppm can be assigned to the aromatic carbons of the -O-$C_6H_4NO_2$ species, which gives the yellow color of this sample.

Acknowledgement

The support of the Army Research Office and the U.S. Army Edgewood Chemical Biological Center, Aberdeen Proving Grounds are acknowledged with gratitude.

  0947-6539/02/0811-2606 $ 20.00+.50/0 *Chem. Eur. J.* **2002**, *8*, No. 11

[1] *Chemistry of Materials* (Ed.: L. Interrante, M. Hampden-Smith), Wiley-VCH, **1998**, Chapter 7, pp. 271–327.
[2] K. J. Klabunde, J. V. Stark, O. Koper, C. Mohs, D. G. Park, S. Decker, Y. Jiang, I. Lagadic, D. Zhang, *J. Phys. Chem. B* **1996**, *100*, 12142–12153.
[3] J. V. Stark, D. G. Park, I. Lagadic, K. J. Klabunde, *Chem. Mater.* **1996**, *8*, 1904–1912.
[4] a) A. Khaleel, P. Kapoor, K. J. Klabunde, *Nanostruct. Mater.* **1999**, *11*, 459–468; b) E. Lucas, K. J. Klabunde, *Nanostruct. Mater.* **1999**, *12*, 179–182.
[5] R. Richards, W. Li, S. Decker, C. Davidson, O. Koper, V. Zaikovski, A. Volodin, T. Rieker, K. J. Klabunde, *J. Am. Chem. Soc.* **2000**, *122*, 4921–4925.
[6] Y. X. Li, J. R. Schlup, K. J. Klabunde, *Langmuir*, **1991**, *7*, 1394–1399.
[7] a) G. W. Wagner, P. W. Bartram, O. Koper, K. J. Klabunde, *J. Phys. Chem. B* **1999**, *103*, 3225–3228; b) G. W. Wagner, O. Koper, E. Lucas, S. Decker, K. J. Klabunde, *J. Phys. Chem. B* **2000**, *104*, 5118–5123; c) With zeolites: G. W. Wagner, P. W. Bartram, *Langmuir*, **1999**, *15*, 8113–8118; d) G. W. Wagner, L. R. Procell, R. J. O'Connor, S. Munavalli, C. L. Carnes, P. N. Kapoor, K. J. Klabunde, *J. Am. Chem. Soc.* **2001** *123*, 1636–1644.
[8] S. Utamapanya, K. J. Klabunde, J. Schlup, *Chem. Mater.* **1991**, *3*, 175–181.
[9] a) K. J. Klabunde, A. Khaleel, D. Park, *High Temp. Mater. Sci.* **1995**, *33*, 99–106; b) M. Grayson, E. J. Griffith, *Topics in Phosphorus Chemistry* Interscience, New York, **1964**; c) M. K. Templeton, W. H. Weinberg, *J. Am. Chem. Soc.* **1985**, *107*, 774–779; d) M. P. Nadler, R. A. Nissan, R. A. Hollins, *Appl. Spectrosc.* **1988**, *42*(4), 634–642; e) R. M. Silverstein, G. C. Bassler, T. C. Morrill, *Spectrometric Identification or Organic Compounds* 4th ed., Wiley, New York, **1981**; f) One reviewer suggested the term "assisted hydrolysis" rather than "destructive adsorption". Since the word hydrolysis indicates a reaction with water, and since water is not involved in these nanoparticle (solid) reactions, we prefer "destructive adsorption". (Although surface-OH groups may be involved, as future work will determine.)
[10] *Phosphorus 31 NMR: Principles and Applications*, (Ed.: D. G. Gorenstein) Academic Press, Orlando, **1984**, Chapter 18, p. 549.
[11] a) M. B. Mitchell, V. N. Sheinker, E. A. Mintz, *J. Phys. Chem. B* **1997**, *101*, 11192–11203; b) T. M. Tesfai, V. N. Sheinker, M. B. Mitchell, *J. Phys. Chem. B* **1998**, *102*, 7299–7302.
[12] A. E. T. Kuiper, J. J. G. M. van Bokhoven, J. Medema, *J. Catal.* **1976**, *43*, 154–167.
[13] S. T. Lin, K. J. Klabunde, *Langmuir*, **1985**, *1*, 600–605.
[14] Y. X. Li, K. J. Klabunde, *Langmuir*, **1991**, *7*, 1388–1393.
[15] G. S. Reddy, R. Schmultzer, *Z. Naturforsch. B* **1970**, *25*, 1199–1214.
[16] N. Sun, Ph.D. thesis, Kansas State University (USA), **1999**.
[17] E. Lucas, S. Decker, A. Khaleel, A. Seitz, S. Fultz, A. Ponce, W. Li, C. Carnes, K. J. Klabunde, *Chem. Eur. J.* **2001**, *7*, 2505–2510.
[18] D. P. Dumas, S. R. Caldwell, J. R. Wild, F. M. J. Raushel, *Biol. Chem.* **1989**, *264*, 19659–19665.
[19] a) N. B. Munro, S. S. Talmage, G. D. Griffin, L. C. Waters, A. P. Watson, J. F. King, V. Hauschild, *Environ. Health Perspect.* **1999**, *107*, 933–974; b) J. Medema, J. J. G. M. van Bokhoven, A. E. T. Kuiper, *NATO Adv. Study Inst. E* **1975**, *13*, 375–389 (CAM 84, 131193).

Received: September 26, 2001
Revised: February 7, 2002 [F3573]